Available online at www.sciencedirect.com
ScienceDirect
Journal of Non-Crystalline Solids 353 (2007) 2557–2566
JOURNAL OF NON-CRYSTALLINE SOLIDS
www.elsevier.com/locate/jnoncrysol

Linear and non-linear optical properties of 2,5-disubstituted pyrroles supported by a catalyst-free SiO_2 sonogel network

Omar G. Morales-Saavedra [a,*], Gloria Huerta [b], Roberto Ortega-Martínez [a], Lioudmila Fomina [b]

[a] *Lab of Nonlinear Optics, Centro de Ciencias Aplicadas y Desarrollo Tecnológico, CCADET-UNAM, Universidad Nacional Autónoma de México, Apartdo Postal 70-186, C.P. 04510, Coyoacán, México, DF, Mexico*

[b] *Departamento de Polímeros, Instituto de Investigaciones en Materiales, IIM-UNAM, Universidad Nacional Autónoma de México, Apartado Postal 70-230, C.P. 04510, Coyoacán, México, DF, Mexico*

Received 21 December 2006; received in revised form 26 March 2007
Available online 4 June 2007

Abstract

The preparation and optical characterization of pyrrole based sol–gel hybrid materials generated by ultrasonic irradiation (Sonogel composites) are presented in this work. Pyrrole compounds were recently synthesized in our group by a modification of the Schulte–Reisch reaction; these molecular systems were dissolved at different concentrations in tetrahydrofuran (THF) and optimally embedded into a catalyst-free SiO_2 sonogel network. For this purpose, we exploited the novel catalyst-free (CF) sonolysis route to produce highly pure sol–gel glasses, generated via sonochemical reactions. This approach has been recently developed in our research group and has been successfully implemented to develop several hybrid composites for optical applications. By this method, homogeneous and stable solid-state hybrid samples suitable for optical characterization can be produced. The high porosity exhibited by the sonogel matrix allowed us to prepare several pyrrole doped composites with variable dopant concentration. The linear and nonlinear optical (NLO) properties of these amorphous hybrid structures were determined by absorption- and photoluminescent (PL)-spectroscopies, and by the optical third harmonic generation (THG) techniques, respectively. The implemented catalyst-free sonolysis route produced SiO_2-host networks of high chemical and optical purity, suitable for optical and photonic applications.

PACS: 71.20.Rv

Keywords: Silicon; Laser–matter interactions; Optical spectroscopy; Porosity; Absorption; Luminescence; Non-linear optics; Polymers and organics; Sol–gel, aerogel and solution chemistry; Organic–inorganic hybrids

1. Introduction

Optics and particularly nonlinear optics have emerged in the last decades as very important research fields providing several high-tech applications in opto-electronics, photonic technologies and optical data processing [1–7]. During the past decade, considerable progress has been made in understanding the factors that affect the molecular and material properties for optical applications, recent investigations have demonstrated that organic materials represent a better alternative for nonlinear optical applications due to their ultrafast response times, lower dielectric constants, better processability characteristics and enhanced NLO-responses [4–7]. On the other hand, the sol–gel technique has been intensively used over the past twenty years as a standard methodology to confine and encapsulate diverse dopant species into glassy networks in order to prepare advanced materials with interesting chemical and physical properties [8–10]. Numerous applications have been

* Corresponding author. Tel.: +52 55 5622 8602x1124; fax: +52 55 5622 8637.
E-mail addresses: omar.morales@ccadet.unam.mx, omardel@gmail.com (O.G. Morales-Saavedra).

0022-3093/$ - see front matter © 2007 Elsevier B.V. All rights reserved.
doi:10.1016/j.jnoncrysol.2007.04.019

proposed in recent years for organic doped SiO_2 porous matrixes in several research fields of nonlinear optics and photonics, where numerous photo-physical effects such as photorefractivity, optical limiting, second and third harmonic generations (SHG, THG), nonlinear refraction, photochromicity; applications to sensing and storage devices, biomedicine and tunable solid-state dye laser systems, among others, have been successfully demonstrated [8–11]. Recently organic–inorganic SiO_2 based sol–gel hybrid composites have been intensively investigated regarding their optical and NLO properties [8,10,12].

The optimal inclusion of organic molecular systems into an amorphous inorganic SiO_2 matrix could generate alternative low-cost solid-state optical materials. Other important aspects to be considered in the development of efficient devices suitable for optical sciences and photonics, are the material malleability and the mechanical stability of the samples, requirements which are necessary in the development of many technological implementations, as for example optical wave guiding systems, where deposition of high quality organic thin films is essential to fill up the corresponding optical channels and circuitry, which have to remain stable for long periods of time [6,13].

From a sol–gel chemistry point of view, the simple material processing offered by the colloidal state, together with current developments on the deposition of doped sol–gel thin film layers could largely satisfy the requirements mentioned above [14]. The SiO_2 gelation process may take a long time for the doped colloidal mixture to reach a dry and stable solid-state, which allows efficient deposition of doped colloidal dispersions (sols) onto the micrometric and integrated structures registered in different kinds of wafers and substrates. The high malleability of these materials means that they can adopt a very wide variety of shapes required for photonic purposes. Once the drying process is completed, the rigidity of the hybrid sol–gel material can be achieved in a desired shape. The constituting organic compounds will contribute with the desired physical or chemical property, whereas the inorganic part of the composite increases the mechanical and thermal strength [15,16]. These materials can show a very stable behavior within a wide range of temperatures depending on the purity of the sol–gel precursor solvents; even the optical properties of the organic dopants can be preserved without decomposition.

In this work, we report the development, linear and nonlinear optical characterization of several 2,5-disubstituted pyrrole based sonogel hybrids; the implemented pyrrole compounds were recently synthesized in our research group by a modification of the Schulte–Reisch reaction [17]. The intrinsical potential of these molecular systems was clearly beyond the initial goal of this work. To the best of our knowledge, the optical properties of this family of compounds have not yet been reported in the literature. Therefore, we used these molecular systems as dopant materials to create solid-state hybrids suitable for optical characterization. For this purpose, we exploited the novel catalyst-free (CF) sonolysis route to produce highly pure sol–gel samples, which are generated via a sonochemical reaction induced by ultrasonic (US) irradiation. This approach has been successfully implemented to develop several hybrid composites for optical applications [18–21]. The sonogel materials obtained by this method exhibit an amorphous SiO_2 matrix with large surface area, high purity and nanometric porosity. These characteristics provide a suitable environment for inclusion of organic chromophores. In order to generate CF-sonogel materials, instead of the use of acidic and basic catalyst, energetic pulsed US-waves are applied to the interface TEOS/H_2O (tetraethyl-orthosilicate/three-distilled water) producing acoustical cavitation. After drying, the formed hybrid composites showed good physical properties, such as micro-structural homogeneity, good mechanical properties (controllable geometry in monolithic structures), high optical quality and high laser damage thresholds, which are appropriate for several optical functions. The use of high dopant concentrations is also possible. The use of novel and highly pure CF-sonogels based on pyrrole compounds has been carried out as a primary and explorative research in the development of photonic organic–inorganic prototypes. The materials described above may provide practical alternatives to expensive inorganic crystals, due to the necessity of low-cost optical chromophores.

2. Experimental section

2.1. Synthesis and modeling of 2,5-disubstituted pyrrole compounds

Organic materials have long been targeted for use in NLO devices [21–27]. The development of such materials primarily depends on the optimization of molecular as well as material NLO-responses. Molecular NLO-response is generally observed in donor–acceptor–π-conjugated systems containing built-in dipole moment. In such molecules, the π conjugation provides a pathway for the distribution of electric charge under the influence of an external electric field, whereas the donor and acceptor substituents provide the required ground-state charge asymmetry (primarily required for quadratic $\chi^{(2)}$ NLO-effects). Experimental [28], and theoretical [29–31] studies have demonstrated that replacing the benzene ring of a chromophore bridge with easily delocalizable five membered heteroaromatic rings as a pyrrole, results in an enhanced molecular polarizability of donor–acceptor compounds, where the pyrrole ring acts as electron-withdrawing structure [32]. Due to their solvatochromic, electrochemical and nonlinear optical properties, donor–acceptor pyrrole derivates could be employed for the manufacture of semiconductor materials or materials with strong NLO-responses [32,33]. Furthermore, pyrrole and oligomers synthesis has increased due to their application as electroluminescent devices [34].

For the present application, diphenyldiacetylene was used as precursor sample (PS or compound **1**) and was

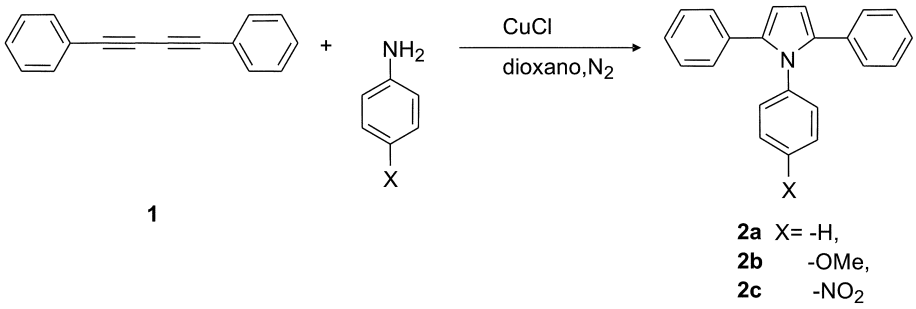

Fig. 1. Chemical reaction of diphenylacetylene with different aromatic amines used to obtain the pyrrole derivatives.

Table 1
Theoretical calculation of the dipole moments of compounds **2a**, **2b** and **2c** in THF-solution and gas phase (all values in Debye) using B3LYP/cc-pvtz(-f)//B3LYP/cc-pvtz(-f) level of theory

Compound	In gas phase (D)	In THF-solution (D)
–H (**2a**)	1.85 ± 0.055	2.29 ± 0.068
–OMe (**2b**)	2.95 ± 0.085	3.56 ± 0.107
$-NO_2$ (**2c**)	3.55 ± 0.106	4.17 ± 0.125

obtained through a modification of Hay's oxidative coupling using copper chloride(I) as catalyst (see Fig. 1) [35]. As shown in Fig. 1, 1,2,5-triphenyl pyrrole (compound **2a**), 1-(*p*-methoxyphenyl)-2,5-triphenylpyrrole (compound **2b**) and 1-(*p*-nitro-phenyl)-2,5-triphenylpyrrole (compound **2c**) were synthesized by the reaction of diphenyldiacetylene with different aromatic amines employing copper chloride(I) as catalysis, the synthesis and characterization of these compounds have been recently described [17]. These compounds were obtained by a modification of a reported procedure [36].

Since the dipole moment (μ) of any organic chromophore plays an important role in the optical performance, the dipole moments of all pyrrole derivatives were estimated theoretically using the Jaguar 6.5 suit of programs (Jaguar 6.0, Schrodinger, LLC, Portland, Oregon, 2005), see Table 1. The geometry of the molecules was optimized using the hybrid B3LYP functional in combination with the cc-pVTZ basis set. If we compare the experimentally measured dipole moments with the theoretical prediction using the largest cc-pVTZ basis sets in combination with Becke3LYP methods, the theoretical method overestimates charge separation in the molecule, producing an estimated error of about 3%. Nevertheless, other combinations of basis sets, quantum mechanical methods, and population analysis methods lead to larger deviations from the experimental values. For example, this level of theory predicts μ of water of 1.96 D in close agreement with experiment (1.85 D, gas phase) [37].

2.2. Preparation of catalyst-free sonogels as host material for 2,5-disubstituted pyrrole compounds

The sol–gel method has been frequently used to synthesize amorphous SiO_2 based on the hydrolysis of different precursors such as TEOS and TMOS, followed by condensation reactions of the hydrolyzed species. This methodology has been widely adopted as a suitable way to obtain glassy doped materials with good optical and mechanical quality. Both hydrolysis and condensation reactions occur normally in the presence of acidic or basic catalysts where ethanol or methanol are commonly used as standard solvents for the precursor and water reactants. Fundamental and experimental details for the sol–gel synthesis of SiO_2 can be found extensively in the literature [8,9]. On the other hand, several articles reporting emulsification of the reactive mixtures induced by ultrasonic irradiation have been published in recent years, where no solvents are used [38–41]. In this way, it is possible to obtain sonolyzed-gel materials with an elastic modulus several orders of magnitude higher than those prepared by conventional methods [42]. In this contribution, a novel approach for the preparation of highly pure SiO_2 sonogels is exploited. In this case, the use of both solvents and catalysts is fully suppressed and the hydrolyzed species are substituted by molecular radicals generated by ultrasound. Extensive details on the synthesis, chemistry and methodology to produce these novel materials can be found in the literature [18,19,21]. In the present report, the catalyst-free sonogel route is implemented to obtain SiO_2 matrices with high optical quality as host materials for novel 2,5-disubstituted pyrrole compounds. As precursor solution 25 mL of tetraethylorthosilicate (TEOS, Fluka 99% purity) and 25 mL of three-distilled water were mixed into a glass vessel and stabilized at 1 °C for 1 h before US-irradiation. A metallic ultrasound tip (Cole-Parmer-CPX, with 1.25 cm in diameter), carefully located at the TEOS/H_2O surface interface, provides an effective irradiation power density on the order of 3.2 W cm^{-3} at 60 Hz. The tip of the ultrasonic-wave generator also acts as an ultrasonic-homogenizer. After 3 h of programmed US-irradiation (on/off-intermittent sequences of 5 s net irradiation time: 1.5 h), the sonicated suspension was kept in the reactor vessel at room conditions for 24 h; thereafter two immiscible phases appear: the upper one, corresponding to unreacted TEOS was removed and eliminated, whereas the lower phase corresponding to a stable colloidal suspension and containing the sonicated induced hydrolyzed product (OH-TEOS) was carefully dropped into cylindrical Teflon-containers

at different volumes. The 2,5-disubstituted pyrrole compounds, previously dissolved in tetrahydrofuran (THF) were afterwards added and ultrasonically mixed to the deposited colloidal suspensions in order to start the inclusion of dopants within the CF–SiO_2 matrix and the formation of bulk hybrid composites.

In the present application, dopant-dissolutions (D-D) containing 8 mg of the 2,5-disubstituted pyrrole compounds and 10 mL of solvent THF were prepared. In this way saturated dissolutions were assured in order to fabricate several highly loaded, optically active sonogel composites. The doses ratio of the OH-TEOS versus the dopant-dissolution (OH-TEOS:D-D) were carefully prepared with a precise volumetric pipe and deposited into the cylindrical Teflon-containers (1 in. in diameter, 2 mL in volume) to obtain different doped optical glasses. Prepared hybrid materials were generated according to the previous methodology with a starting total volume of 2 mL, varying the OH-TEOS:D-D concentration ratio (in volume) as follows: 1.0:1.0, 1.2:0.8, 1.3:0.7, 1.4:0.6, 1.5:0.5, 1.6:0.4, 1.7:0.3 and 1.8:0.2 mL. Undoped or pure reference (PR)-sonogel samples (2:0) were also prepared for reference and calibration purposes. The samples were isolated while drying with a plastic cover in order to avoid atmosphere and temperature variations, and conserved for two to three weeks at room conditions in closed recipients with a small hole in the cap in a clean-dry-dark environment. Rigid and geometrical monolith shape samples adequate for optical characterization were obtained after this slow drying process. The resulting bulk hybrids possess higher purity compared to other traditional synthesized sol–gel hybrid composites, because the use of the US-waves instead of reactive solvents and catalyst, gives samples with higher optical quality [18,19]. The bulk samples, generally obtained for very slow drying speeds, showed monolithic cylindrical shapes with diameters and thickness varying from 8 to 12 mm and 0.5 to 1.7 mm, respectively.

It has been noted that solutions of dopants in THF are better incorporated into the CF-sonogel network, since the S_4 geometry of TEOS implies a zero dipolar moment and would not accept the inclusion of highly polar THF-based dissolutions. However, the OH-TEOS group is highly polar too, and provides an optimal environment for molecules dissolved in THF (dipolar moment: $\mu = 1.6$ D).

2.3. Linear and nonlinear optical characterization

Pyrrole compounds and the precursor diphenylacetylene were dissolved in spectrophotometrical grade THF purchased from Aldrich. UV–vis absorption spectra of these compounds in solution (using 1 cm quartz cells) and in sol–gel were recorded at room temperature within the 200–1100 nm spectral range on a double beam Shimadzu-260 UV–vis spectrophotometer, taking air in the reference beam. Similarly, PL-measurements were obtained in the 200–900 nm spectral range with a FluoroMax-3, Jobin-Yvon-Horiba fluorimeter. Excitation wavelengths were selected according to the UV–vis absorption spectra of the liquid or solid-state hybrid samples to a convenient wavelength (near the absorption wavelength maximum) for each case.

The amorphous solid-state sonogel hybrid composites were also studied as active media for cubic $\chi^{(3)}$-nonlinear optical effects such as THG, from where the complex value of the non-degenerated $\chi^{(3)}(-3\omega;\omega,\omega,\omega)$ coefficient, and the intensity dependent refractive index (IDRI or n_2: degenerated Re $[\chi^{(3)}(-\omega;\omega,-\omega,\omega)]$ coefficient) were evaluated [43]. An advantage of the THG technique is that the THG-response accounts only for the ultrafast electronic response, so that vibrational, orientational, and thermal effects, which may contribute to the overall nonlinear optical response of the material, are excluded. The THG experimental device is schematically shown in Fig. 2, where a commercial Q-switched Nd:YAG Laser system (Surelite II from Continuum, $\lambda_\omega = 1064$ nm, repetition rate of 10 Hz and a pulse width of $\tau \approx 12$ ns) was implemented to provide the fundamental wave. Typical pulse powers of 200 μJ were filtered in order to irradiate the samples by means of an $f = 50$ mm focusing lens, thus peak irradiances on the order of 30–40 MW cm^{-2} were achieved at the focal spot on the hybrid samples. This value was slightly below the damage threshold energy supported by the samples under strong focused beam irradiation. The polarization of the fundamental beam (S or P polarizing geometry) was selected by means of an IR-coated Glan-Laser polarizer and a $\lambda/2$-Quarz-retarder. A second polarizer, used as an analyzer allowed the characterization of the THG-response. The third harmonic wave ($\lambda_{3\omega} = 355$ nm) was detected by a sensitive photomultiplier tube (HAM-

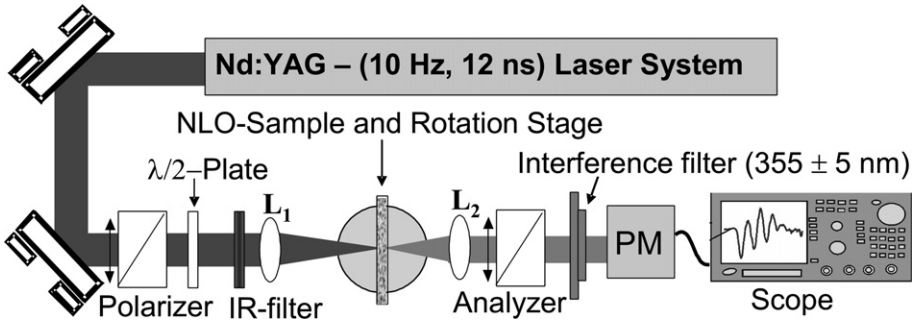

Fig. 2. Experimental device used for NLO–THG measurements in pyrrole based sonogel hybrid materials.

AMATSU R-928) placed behind interference optical filters centered at 355 ± 5 nm. The THG-device was previously calibrated by means of a fused silica plate ($\chi^{(3)} \approx 3.11 \times 10^{-14}$ esu, at $\lambda_\omega = 1064$ nm), which is frequently used as a NLO-reference standard via the Maker-Fringes method [1,3,5,44–47].

3. Results

3.1. Linear optical properties in solution and sol–gel phase

The linear optical properties of the precursor diacetylene **1** (precursor sample: PS) and the different 2,5-disubstituted pyrroles (**2a**, **2b** and **2c**) were studied in THF-solutions and the sol–gel phase by linear absorption spectroscopy within the UV–vis–NIR spectral region and the respective results are shown in Figs. 3 and 4. As shown in Fig. 3(a), unsaturated THF-solutions (2.5 mg, of the 2,5-disubstituted pyrrole compounds and 11 mL of THF-solvent) were prepared in order to assure that the Beer–Lambert law applies in such partially transparent solutions; hence the electronic spectra and absorption properties of the different 2,5-disubstituted pyrroles were easily recognized (see Table 2). On the other hand, Fig. 3(b) shows the saturated absorption spectra of the same compounds dissolved in THF as they were used to produce highly loaded sonogel hybrids (8 mg: 10 mL). These samples, as will be shown below, were also studied under strong laser irradiation in order to estimate their NLO-properties. In this context, the available laser excitation line (at $\lambda_\omega = 1064$ nm) and the line at the THG wavelength ($\lambda_{2\omega} = 355$ nm) are shown in these figures.

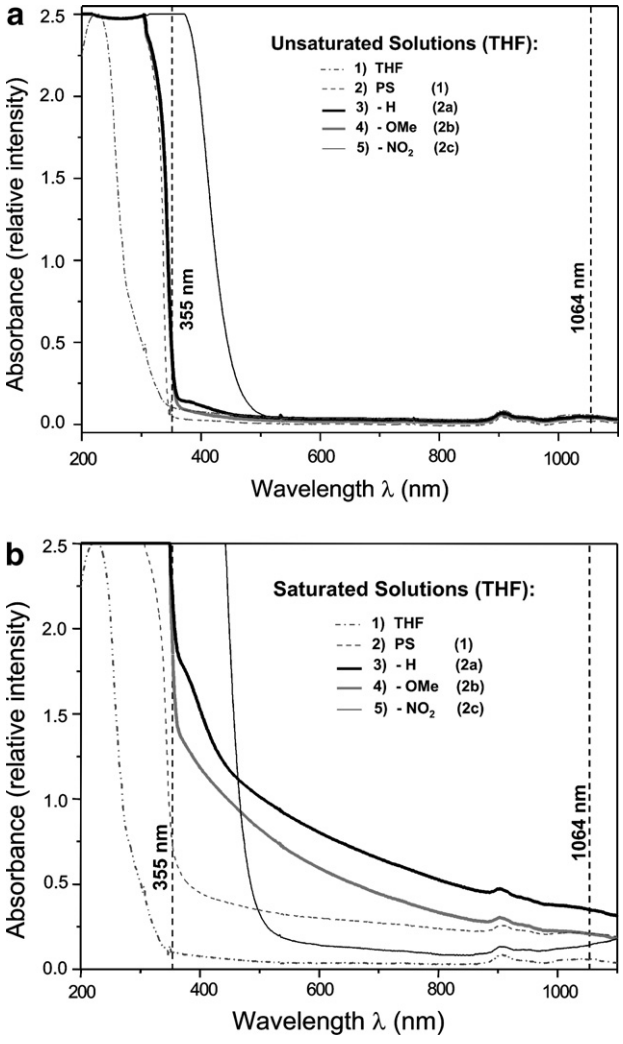

Fig. 3. Comparative absorption spectra of (a) unsaturated THF-solutions and (b) saturated THF-solutions for the precursor sample (PS or **1**), compound **2a**, compound **2b** and compound **2c**.

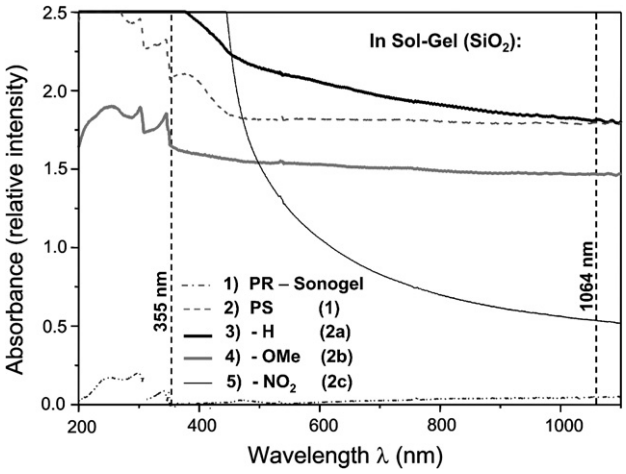

Fig. 4. Comparative absorption spectra between a (2.0:0.0) pure reference PR-sonogel glass and several (1.6:0.4)-pyrrole doped composites: (1) PR-sonogel, (2) Precursor sample (PS or **1**), (3) **2a**-based hybrid, (4) **2b**-based hybrid, and (5) **2c**-based hybrid.

Comparative photoluminescence spectra studies of the diacetylene precursor sample (PS) and the different 2,5-disubstituted pyrroles in THF-solution and in sol–gel phase were also carried out and their respective electronic spectra are also summarized in Table 2. Fig. 5 shows comparative PL-spectra (not normalized) between the PS-sample (in sol–gel phase and THF-solution) and the PR-glass sample. Similarly, Figs. 6–8 show the comparative PL-spectra (not normalized) of the different 2,5-disubstituted pyrroles (**2a**, **2b** and **2c**) in THF-solution and in sol–gel phase, respectively.

3.2. Nonlinear optical properties in sol–gel phase

Here we report the cubic NLO-properties of the developed hybrid structures. Since the amorphous sol–gel phase exhibits an isotropic and centro-symmetric-like network arrangement, no crystalline and symmetry conditions are required for the observation of cubic $\chi^{(3)}$ NLO-effects [1,3,5–7]. On the other hand, experimental single beam techniques based on THG give direct access to the cubic $\chi^{(3)}$ nonlinear optical coefficient, which is completely determined by the ultra-fast electronic response. Thus,

Table 2
Linear and nonlinear optical data obtained from samples PR, PS:**1**, **2a**, **2b** and **2c** in THF-solutions and in sol–gel phase

Sample	λ_{max} – Absorbance (nm)		λ_{max} – PL (nm)		$\chi^{(3)}$ (THG) $\times 10^{-12}$ (esu)	n_2 – Values $\times 10^{-10}$ (esu)
	Unsaturated THF-solution	Sol–gel hybrid phase	THF-solution	Sol–gel hybrid phase	Sol–gel hybrid phase	Sol–gel hybrid phase
Pure sonogel (PR)	–	340	–	413	0.3 ± 0.06	4 ± 0.6
Precursor sample (PS)	300	240	398	423	22 ± 4	18 ± 2
THF-solvent	225	–	378	–	–	–
Compound –H (**2a**)	300	370	387	409	38 ± 8	61 ± 7
Compound –OMe (**2b**)	300	351	382, 753	411, 485, 842	55 ± 13	114 ± 14
Compound –NO_2 (**2c**)	300–375	445	520	449	78 ± 16	145 ± 22

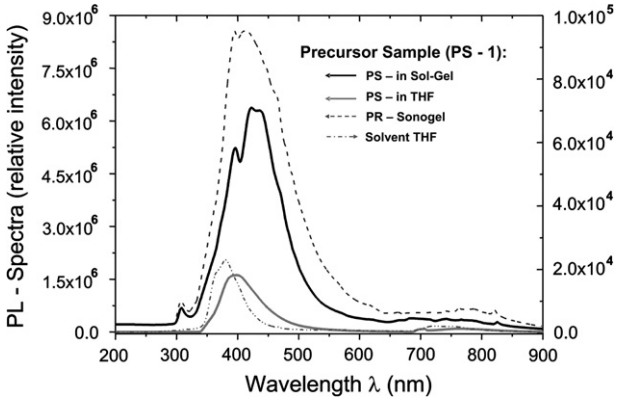

Fig. 5. Comparative PL-spectra obtained for a PR-sonogel sample (2.0:0.0, $\lambda_{ex} = 250$ nm), a PS doped composite (1.6:0.4, $\lambda_{ex} = 350$ nm), compound PS dissolved in THF ($\lambda_{ex} = 350$ nm) and solvent THF ($\lambda_{ex} = 250$ nm).

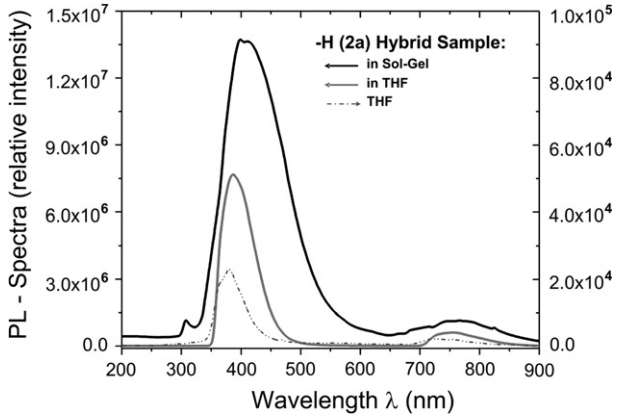

Fig. 6. Comparative PL-spectra obtained for a **2a** sonogel doped composite (1.6:0.4, $\lambda_{ex} = 350$ nm), compound **2a** dissolved in THF ($\lambda_{ex} = 350$ nm) and solvent THF ($\lambda_{ex} = 250$ nm).

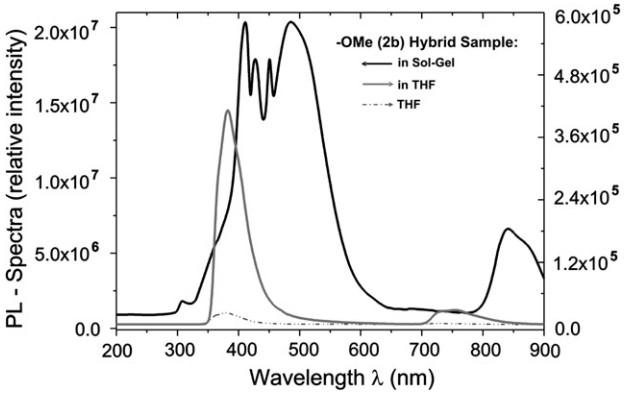

Fig. 7. Comparative PL-spectra obtained for a **2b** sonogel doped composite (1.6:0.4, $\lambda_{ex} = 350$ nm), compound **2b** dissolved in THF ($\lambda_{ex} = 250$ nm) and solvent THF ($\lambda_{ex} = 250$ nm).

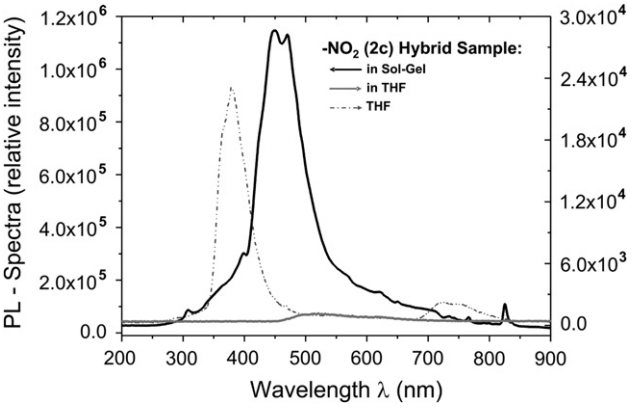

Fig. 8. Comparative PL spectra obtained for a **2c** sonogel doped composite (1.6:0.4, $\lambda_{ex} = 350$ nm), compound **2c** dissolved in THF ($\lambda_{ex} = 350$ nm) and solvent THF ($\lambda_{ex} = 250$ nm).

vibrational, orientational, and thermal effects, which may contribute to the overall non-linear response of the material, are excluded. For these reasons and according to Bloom et al. [43], we implemented the THG-technique, in order to evaluate the complex value of the non-degenerate $\chi^{(3)}(-3\omega;\omega,\omega,\omega)$ cubic nonlinear coefficient, which can additionally be related to the degenerate $\chi^{(3)}(-\omega;\omega,-\omega,\omega)$ component in order to give a good estimate of the intensity dependent refractive index (IDRI or n_2): Re$[\chi^{(3)}(-\omega;\omega, -\omega,\omega)]$.

In Fig. 9(a), we report typical Maker-fringe pattern experiments (THG-resonant configuration: $\lambda_\omega = 1064$ nm, $\lambda_{3\omega} \sim 355$ nm, normalized intensity) of moderated doped 1.6:0.4 and ~0.65 mm thick PS- and 2,5-disubstituted pyrrole based hybrids. The Maker-fringe signals of the hybrid systems are compared to the fine fringe pattern produced by the PR-sample (see Fig. 9(b)) and the standard refer-

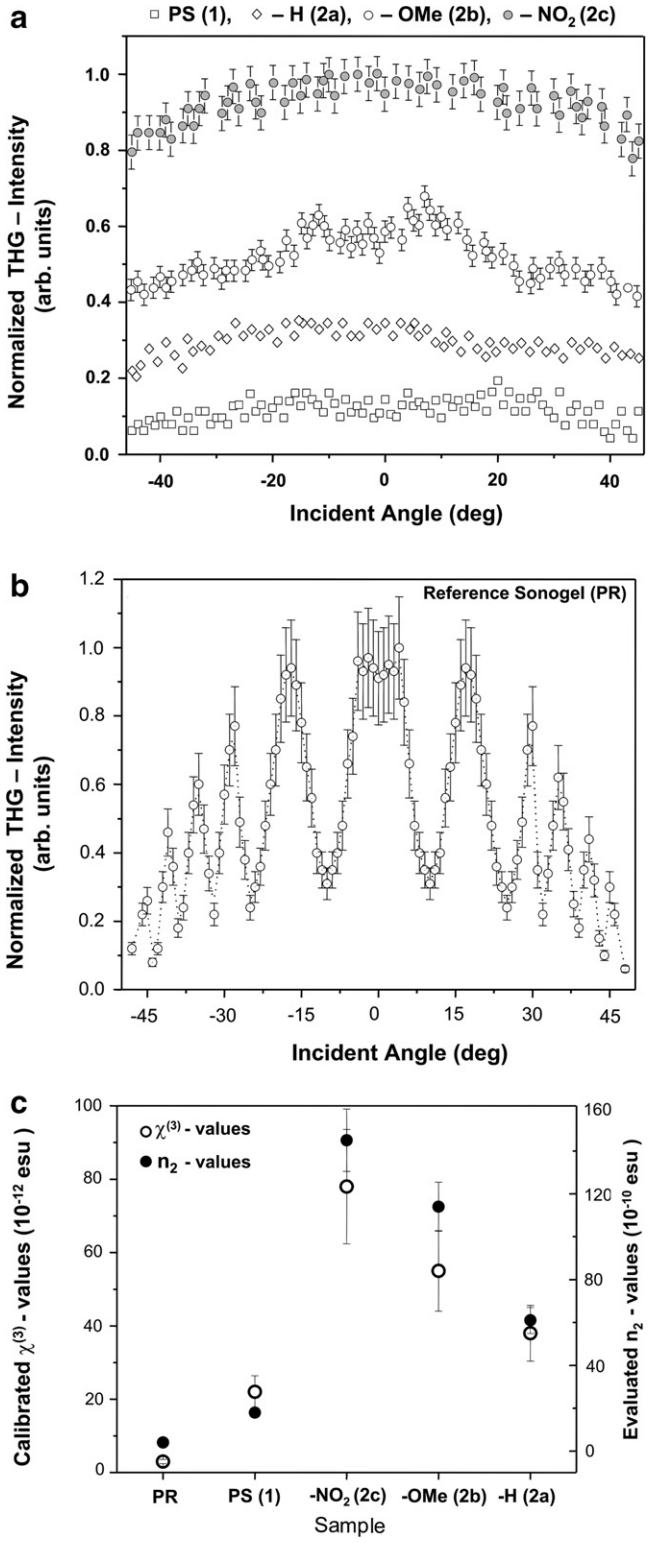

Fig. 9. Angle dependent THG-measurements performed in (a) hybrid solid-state samples (1.6:0.4 – PS sonogel and 1.6:0.4 – pyrrole doped composites) and (b) a 2.0:0.0 – PR sonogel. Measurements were performed implementing experimental P-In/P-Out polarizing geometries. (c) Calibration of the $\chi^{(3)}(-3\omega;\omega,\omega,\omega)$ and n_2 coefficients.

ence. Intensities in Fig. 9(a) and (b) are normalized independently to a maximum value, however a magnifying factor of 6.6×10^{4} should be applied to the THG-intensity scale of Fig. 9(a) when comparing to the values displayed in Fig. 9(b). Estimated experimental error bars have been included in all graphs. Such systematic errors have been evaluated depending on the sensitivity of the instruments used (photomultiplier, oscilloscope, power-meter and photodiodes). In the cases of samples **1** and **2a** (see Fig. 9(a)), the error bars are smaller than the size of the symbols used.

As a first estimation of the cubic NLO-properties of these hybrid composites, considering samples under strong resonant (absorption) conditions, the determination of $\chi^{(3)}$ may be approximated by the following expression [53]:

$$\chi^{(3)\text{-Hybrid}} \propto \chi^{(3)\text{-reference}} \left(\frac{2l_c^{\text{reference}}}{\pi}\frac{\alpha/2}{1-e^{-\alpha/2}}\right)\left(\frac{I_{3\omega}^{\text{Hybrid}}}{I_{3\omega}^{\text{reference}}}\right)^{1/2}, \quad (1)$$

where α is the absorption coefficient of the hybrid sample and $l_c^{\text{reference}}$, represents the coherence length of the reference material ($\sim$7 μm). $\chi^{(3)\text{-Hybrid}}$ and $\chi^{(3)\text{-reference}}$ are, respectively, the values of the cubic nonlinear coefficients of the doped samples and the fused silica plate, while $I_{3\omega}^{\text{Hybrid}}$ and $I_{3\omega}^{\text{reference}}$ are the peak intensities of the Maker-fringe patterns of both the hybrid sample and the reference plate. In this way, the $\chi^{(3)}$ value of a new material relative to the value of the reference standard can be obtained; hence a calibrated result with a high degree of accuracy can be reported.

Assuming that the doping agents are homogeneously dispersed within the SiO_2 sonogel matrix and since no quadratic SHG signals were measured in our samples, only cubic $\chi^{(3)}$ resonant enhancements are permitted in such amorphous systems, therefore the THG-process is completely dominated by three-photon resonances $\chi^{(3)}(-3\omega;\omega,\omega,\omega)$ and no cascading effects were considered [5,54]. From the Maker-fringe experiments, the cubic NLO coefficients for the hybrid samples were evaluated according to Eq. (1) to be $\chi^{(3)}_{-NO_2} = 78\times10^{-12}$ esu, $\chi^{(3)}_{-OMe} = 55\times10^{-12}$ esu and $\chi^{(3)}_{-H} = 38\times10^{-12}$ esu (1.1×10^{-18}, 7.6×10^{-19} and 5.3×10^{-19} $m^2\,V^{-2}$, respectively) and are graphically represented in Fig. 9(c) for the selected H-TEOS:D-D concentration, where an estimated experimental error of about 20% is considered. The calibrated nonlinear $\chi^{(3)}$-optical coefficients were obtained from a direct comparison between the maximal THG-intensities observed from the Maker-fringe experiments of the reference material and the hybrid composites (see Fig. 9(a) and (b)) and evaluated according to Eq. (1). The obtained $\chi^{(3)}$-coefficients, were the highest among the studied doped samples and are considerably larger than those measured for the pure reference sonogel (PR) and the precursor based hybrid sample (PS): $\chi^{(3)}_{PR} = 0.3\times10^{-12}$ esu and $\chi^{(3)}_{PS} = 22\times10^{-12}$ esu (4.2×10^{-21} and 3.1×10^{-19} $m^2\,V^{-2}$, respectively). All $\chi^{(3)}$-values were measured at room temperature for samples with the same thickness, and these measurements reveal an optimal concentration between the H-TEOS and the 2,5-disubstituted pyrrole-doped solutions in order to obtain best possible THG among the prepared hybrids. The moderate 1.6:0.4

NO_2-based hybrids exhibited a $\chi^{(3)}$-coefficient about 260 and 3.6 times larger than those measured for the PR- and PS-composites, respectively.

According to Bloom et al. [43], the intensity dependent refractive index (IDRI or n_2) for the solid-state doped samples considered in this work, were also evaluated. Their respective n_2-values are plotted in Fig. 9(c) and tabulated in Table 2. Here, the uncertainties for the evaluated $\chi^{(3)}(-3\omega;\omega,\omega,\omega)$ and n_2 values have been included; this evaluation follows traditional uncertainty evaluation and statistical procedures applied to experimental data, to Eq. (1) and to the theoretical procedures given by Bloom et al. [43].

4. Discussion

4.1. Linear optical properties in solution and sol–gel phase

It is interesting to note from the electronic spectra of the different 2,5-disubstituted pyrroles recorded in THF-solution and in sol–gel (see Table 2), that the pyrrole compounds depicted in Fig. 1 have different photo-physical properties depending on their molecular structure. In general, as can be seen from Fig. 3, samples **1**, **2a** and **2b** in unsaturated THF-solutions are nearly transparent within the vis–IR and highly absorptive in the UV. Sample **2c** exhibits a broader absorption band from the UV region up to about 500 nm, which indicate a higher conjugation degree for this molecular system as was explored and confirmed by means of NLO–THG experiments. The precursor diacetylene (**1**) shows a strong band in THF-solution in the high energy UV-region at ~300 nm, whereas pyrrole derivatives exhibit an intense absorption band in the UV–vis region attributed to the σ–σ^* transitions of the conjugated system, which can be observed in both saturated solutions and sol–gel phase (see Fig. 4). By contrast, due to its high purity level, the absorption spectra of a pure sonogel sample (2.0:0.0 or pure reference: PR) showed only small absorption bands within the 240–340 nm UV spectral range [19], these bands are significantly less intense than those observed for the doped composites and represent typical features of SiO_2 based glassy materials. Thus, it can be assured that the absorption bands observed for the hybrid composites are mainly due to the organic part and that the sonogel matrix does not appreciably contribute to the absorption spectrum of the hybrids. Since in the solid-state the molecular concentration is higher (although relatively lightly 1.6:0.4 doped samples were selected for absorption experiments in solid-state), the absorption spectra of the sol–gel doped samples are remarkably more intense within the visible region than their counterparts in the saturated THF-dissolutions.

In general, the absorption bands of the PS (**1**) and **2a**–**c** molecules were faintly red shifted in the solid-state with respect to THF-solutions (see Table 2), presumably due to the higher polarity in the sol–gel matrix (obtained from OH-TEOS) and to aggregation phenomena which are typically observed in the solid-state. This last fact also reveals that in this media these polymers are better aligned to planarity, this phenomenon can be partially explained in terms of the viscosity of the environment: in solution, polymer molecules can freely move and display rotations, whereas in the sol–gel phase they reach their optimal conformation during the drying process; once the sol–gel matrix is completely dry, the rigidity of the media restrains the molecular mobility, preventing them from adopting other conformations. The inductive electron-donor or electron-withdrawing effect can be evaluated by comparing the λ_{max} values; from the UV spectra in the sol–gel phase it can be noticed that there is a bathochromic effect in the absorption maxima between the nitro group in comparison with the methoxy group ~75 nm. The presence of the electron-withdrawing group stabilizes LUMO, and the maximal absorption band is red shifted, indicating a narrowing in the HOMO–LUMO energy gap (see Table 2).

Concerning the photoluminescent experiments, it is observed from Fig. 5 and Table 2, that the pure reference PR-sample exhibits the highest PL-emission peak around $\lambda_{max} = 413$ nm, characteristic of SiO_2 based glasses (dashed line, excitation line was set to $\lambda_{ex} = 250$ nm) [19], whereas the lightly PS-doped composite shows slightly smaller PL-intensity emission in the same spectral range, presenting a second smaller adjoined band (thick solid line in black, $\lambda_{max} = 423$ nm). In general, the fluorescence emission was increased in the sol–gel matrix in comparison with the emission detected in THF-solution. This behavior may be surprising since photoluminescent organic chromophores are usually less emissive in the solid-state than in solution, due to molecular aggregation forming less emissive species such as excimers [48–51]. However, these observations can be understandable noting the wide high-transmission window (negligible absorption) displayed by the pure reference PR-sonogel within the whole vis–NIR range (see Fig. 4). Thus, the high optical and chemical purity levels displayed by the transparent PR-sonogel network allows maximal bulk PL-emission with minimal volumetric self-absorption effects for this pristine sample, such absorptive effects are clearly present for the thick PS-doped glass and the THF-dissolution (a detailed description of the PL-spectra of PR-sonogels and its characteristics can be found in reference [19]). Furthermore, due to the lower concentration of the PS in THF-solution, the PL-emission is considerably less intense than its solid-state counterpart, and only one band was resolved (thick solid line in gray, $\lambda_{max} = 398$ nm). Similarly to absorption measurements, the PL-spectrum of this compound is significantly red shifted in the solid-state with respect to that detected in THF-solution. Since all four emission spectra shown in Fig. 5 are reasonably similar in shape, with maximal emission bands nearly in the same spectral range, while the stronger PL-emission of the PR-network may overshadow some structural details of the PS-doped glass, we can only argue that the observed spectral red shift is in principle more related to the tendencies induced by the peak PL-

bands of the THF-solvent (dot-dashed line) and the PR-host matrix, in their respective PS-doped phases.

The comparative PL-spectra of the different 2,5-disubstituted pyrroles (**2a**, **2b** and **2c**) shown in Figs. 6–8, illustrate that the maximal emission bands detected in these compounds were again stronger in the solid-state than in THF-solutions. In the case of polymers **2a** and **2b** (Figs. 6, 7), the maximal PL-bands were once more significantly red shifted in the solid-state with respect to that of the THF-solutions (see also Table 2). As can be seen from the PL-spectra of these doped glasses, the emission intensities were at least an order of magnitude higher than that measured for a PR-sample (see Fig. 5); hence the weaker emission of the PR-glass does not significantly modify the emission spectra of these doped samples in this case. PL-spectrum of compound **2b** in solid-state differs considerably from that observed in THF-solution; here the main emission band is divided into two well-defined minor emission peaks (see Table 2), which probably result from stronger molecular interactions of this structure at the organic–inorganic porous interfaces. Further experiments will be necessary in order to clarify this last fact. Fig. 8 shows the PL-spectra of pyrrole **2c**, this polymer shows weaker PL-activity (in solution and in sol–gel) than compounds **2a** and **2b**, its respective PL-bands are less intense than those observed for the PR-sonogel and the PS-doped sonogel. Contrary to compounds **2a** and **2b** the main PL-band observed in THF-solution is now red shifted with respect to that detected in the solid-state (see Table 2); this fact could be attributed to a restriction in the molecular rotation, which makes a large contribution to the non-radiative transition process in solution [52].

4.2. Nonlinear optical properties in sol–gel phase

From Fig. 9(a) and (b), it is clear that the THG-signals obtained from the hybrid composites do not show any significant oscillating behavior and the THG-responses produced by the hybrid composites are considerably stronger than those observed for the PR-sample and the fused silica plate used as NLO-reference standard ($\chi^{(3)} \approx 3.11 \times 10^{-14}$ esu, at $\lambda_\omega = 1064$ nm). The lack of sharp oscillations for the hybrid systems is due to the resonant conditions occurring in our experiments using the available laser source, where the generated THG free waves at $\lambda_{3\omega} = 355$ nm are highly absorbed by the huge amount of NLO-chromophores embedded into the SiO_2 network (see Fig. 4); hence, the THG-intensity will no longer follow the typical phase-matching dependent oscillations with the medium thickness, according to the Maker-fringe experiments. For the PR-sample, absorption is negligible and thus a fine fringe pattern can be easily recognized.

According to Table 1, the implemented theoretical method predicted a higher μ value for the nitro derivative (sample **2c**); such theoretical evaluations correlate well with the experimental results obtained from THG experiments, which can be explained by the higher inductive electron-withdrawing effect of the nitro substituent. Finally, the theoretical evaluation of the intensity dependent refractive index (IDRI or n_2), evaluated for the solid-state samples (see Table 2), are likewise well correlated to the $\chi^{(3)}(-3\omega;\omega,\omega,\omega)$ coefficients: again, the NO_2-based composite exhibits the highest n_2 nonlinear refraction, followed by the –OMe, –H, PS and PR based materials, respectively.

5. Conclusions

The preparation of novel hybrid sol–gel composites based on 2,5 disubstituted pyrroles has been described in this work. These compounds were successfully used in THF-dissolutions as dopant agents in order to fabricate advanced organic–inorganic hybrid composites following the CF-sonogel route. The adequate purity level displayed by the sonogel glasses and the stable mechanical behavior achieved by this method, allowed us to obtain rigid doped materials with convenient geometrical shapes, which were optimal to perform optical characterizations and evaluate several photo-physical properties in the solid-state. Results showed that the tuning of the electronic properties of pyrroles with different substituents in the N center is a key point toward the development of novel ð-conjugated materials. The current study was carried out in the described pyrrole family in order to determine variations in the linear and cubic NLO-values of these molecular systems as functions of their respective dipolar moments and conjugation degree. In fact, and according to theoretical calculations, best third order NLO performance was experimentally evaluated for the NO_2 (sample **2c**) based pyrrole composite, which exhibited the highest $\chi^{(3)}(-3\omega;\omega,\omega,\omega)$ and n_2 values in the interesting range of 10^{-11} and 10^{-8} esu, respectively.

This research work has been carried out as a first and explorative study toward the development of photonic organic–inorganic devices, implementing pyrrole derivative based hybrid sonogel composites. In future work, it will be necessary to improve the SiO_2-sonogel:chromophore concentrations, and the cubic NLO-response. NLO-investigations using other laser sources will also be necessary in order to identify better condition for THG and nonlinear refraction, under non-resonant experimental conditions. To this end, several studies to obtain the dispersion of $\chi^{(3)}$ over a wider spectral range, including the IR spectral region (from 1.2 to 2.0 μm) are currently underway. Such investigations may be interesting for the development of optical communication devices and will be presented elsewhere.

Acknowledgments

We are grateful to José Ocotlan Flores-Flores (CCA-DET-UNAM) for his scientific and technical advice during the sonogel sample preparation and to Miguel A. Canseco-Martinez (IIM-UNAM) for technical support. This work was financially supported by PAPIIT-DGAPA-UNAM

under Project Grant: IN-112703 and SEP-CONACyT under Project Grant: 47421.

References

[1] R.W. Boyd, Nonlinear Optics, Academic, 1992.
[2] B.E.A. Saleh, M.C. Teich, Fundamentals of Photonics, Wiley, 1991.
[3] P.N. Prasad, D.J. Williams, Introduction to Nonlinear Optical. Effects in Molecules and Polymers, John Wiley, 1991.
[4] C.N.R. Rao (Ed.), Chemistry of Advanced Materials, Blachaell Scientific Publications, 1993.
[5] H.S. Nalwa, S. Miyata (Eds.), Nonlinear Optics of Organic Molecules and Polymers, CRC, 1997.
[6] F. Kajzar, J.D. Swalen (Eds.), Organic Thin Films for Waveguiding Nonlinear Optics, Gordon & Breach Publishers, 1996.
[7] D.S. Chemla, J. Zyss, Nonlinear Optical Properties of Organic Molecules and Crystals, Academic, 1987.
[8] S. Sakka (Ed.), Handbook of Sol–Gel Science and Technology: Processing Characterization and Applications, vol. 1–3, Kluwer Academic, 2005.
[9] C.J. Brinker, G.W. Scherer, Sol–Gel Science: The Physics and Chemistry of Sol–Gel Processing, Academic, 1990.
[10] M.P. Andrews, S.I. Najafi (Eds.), Sol–Gel Polymer Photonic Devices: Critical Reviews Optical Science and Technology, SPIE-Optical Engineering Press, 1997, CR68.
[11] D. Levy, Chem. Mater. 9 (1997) 2666.
[12] J.P. Boilot, J. Biteau, F. Chaput, T. Gacoin, A. Brun, B. Darracq, P. Georges, D. Levy, Pure Appl. Opt. 7 (1998) 169.
[13] G. Priebe, K. Kunze, F. Kentischer, R. Schulz, O. Morales, R. Macdonald, H.J. Eichler, 45th SPIE Annual Meeting, vol. 4107, ISBN 0-8194-3752-2, 2000, p. 9.
[14] C. Sanchez, B. Leveau, Pure. Appl. Opt. 5 (1996) 689.
[15] G.L. Wilkes, B. Orler, H.H. Huang, Polym. Prep. 26 (1985) 300.
[16] A. Morikawa, Y. Iyoku, M. Kakimoto, Y.J. Imai, Mater. Chem. 26 (1992) 79.
[17] G. Huerta, L. Fomina, L. Rumsh, M.G. Zolotukhin, Polym. Bull. 57 (2006) 433.
[18] J.O. Flores-Flores, J.M. Saniger, J. Sol–Gel Sci. Technol. 39 (2006) 235.
[19] O.G. Morales-Saavedra, E. Rivera, J.O. Flores-Flores, R. Castaneda, J.G. Banuelos, J.M. Saniger, J. Sol–Gel Sci. Technol. 41 (2007) 277.
[20] O.G. Morales-Saavedra, R. Castaneda, M. Villagran-Muniz, J.O. Flores-Flores, J.G. Banuelos, J.M. Saniger, E. Rivera, Mol. Cryst. Liq. Cryst. 449 (2006) 161.
[21] O.G. Morales-Saavedra, E. Rivera, Polymer 47 (2006) 5330.
[22] M. Won-Junk, Y. Gun Shul, J. Ho Mun, T. Wada, Mol. Cryst. Liq. Cryst. 247 (1994) 111.
[23] V.P. Rao, A.K.Y. Jen, K.Y. Wong, K.J. Drost, Tetrahedron Lett. 34 (1993) 1747.
[24] A.K.Y. Jen, V.P. Rao, K.Y. Wong, K.J. Drost, J. Chem. Soc., Chem. Commun. 1 (1993) 90.
[25] V.P. Rao, A.K.Y. Jen, K.J. Drost, J. Chem. Soc., Chem. Commun. 14 (1993) 1118.
[26] S.S.P. Chou, D.J. Sun, H.C. Lin, P.K. Yang, Tetrahedron Lett. 37 (1996) 7279.
[27] C.F. Shu, W.J. Tsai, J.Y. Chen, A.K.Y. Jen, Y. Zhang, T.A. Chen, J. Chem. Soc., Chem. Commun. 19 (1996) 2279.
[28] A. Facchetti, L. Beverina, M.E. van der Boom, E.G. Dutta, G.A. Pagani, T.J. Marks, J. Am. Chem. Soc. 128 (2006) 2142, and references cited therein.
[29] P.R. Varanasi, A.K.Y. Jen, J. Chandrasekhar, I.N.N. Namboothiri, A. Rathna, J. Am. Chem. Soc. 118 (1996) 12443.
[30] I.D.L. Albert, T.J. Marks, M.A. Ratner, J. Am. Chem. Soc. 119 (1997) 6575.
[31] E.M. Breitung, C.F. Shu, R.J. McMahon, J. Am. Chem. Soc. 122 (2000) 1154.
[32] M.M.M. Raposo, A.M.R.C. Sousa, A.M.C. Fonseca, G. Kirsch, Tetrahedron 61 (2005) 8249.
[33] M.M.M. Raposo, A.M.R.C. Sousa, G. Kirsch, F. Ferreira, M. Belsey, E. de Matos Gomes, A.M.C. Fonseca, Tetrahedron 61 (2005) 11991.
[34] Y. Sakon, T. Ohnuma, M. Hashimoto, S. Saito, T. Tsutsui, C. Adachi, US Patent, 5, 077,142 A, 19, 911, 231, CA 117: 16862, 1991.
[35] A.S. Hay, J. Org. Chem. 27 (1962) 3320.
[36] J. Reisch, K.B. Schulte, Angew. Chem. 73 (1961) 241.
[37] (a) A.D. Becke, J. Chem. Phys. 98 (1993) 5648;
(b) A.D. Becke, J. Chem. Phys. 96 (1992) 2155;
(c) A.D. Becke, J. Chem. Phys. 97 (1992) 9173;
(d) C. Lee, W. Yang, R.G. Parr, Phys. Rev. B 37 (1988) 785;
(e) D.E. Woon, T.H. Dunning, J. Chem. Phys. 98 (1993) 1358;
(f) R.A. Kendall, T.H. Dunning, R.J. Harrison, J. Chem. Phys. 96 (1992) 6796;
(g) F. Martin, H. Zipse, J. Comput. Chem. 26 (2005) 97.
[38] K.S. Suslick, Science 247 (1990) 1373.
[39] N. de la Rosa-Fox, L. Esquivias, J. Zarzycki, Diffus. Defect Data 363 (1987) 53.
[40] K.S. Suslick, Adv. Organomet. Chem. 25 (1986) 73.
[41] B.E. Noltingk, E.A. Neppiras, Proc. Phys. Soc. B 63 (1950) 674.
[42] L. Esquivias, N. de la Rosa-Fox, J. Sol–Gel Sci. Technol. 26 (2003) 651.
[43] F.C. Bloom, A. Driessen, H.J.W.M. Hoekstra, J.B.P. van der Schoot, Th.J.A. Poma, Opt. Mater. 12 (1999) 327.
[44] P.D. Maker, R.W. Terhune, M. Nisenoff, C.M. Savage, Phys. Rev. Lett. 8 (1962) 21.
[45] H.Y. Zhang, X.H. He, Y.H. Shih, M. Schurman, Z.C. Feng, R.A. Stall, Appl. Phys. Lett. 69 (1996) 2953.
[46] N.A. Sanford, A.V. Davydov, D.V. Tsvetkovand, A.V. Dmitriev, S. Keller, U.K. Mishra, S.P. Den Baars, S.S. Park, J.Y. Han, R.J. Molnar, J. Appl. Phys. 97 (2005) 053512.
[47] V. Gopalan, N.A. Sanford, J.A. Aust, K. Kitamura, Y. Furukawa, Handbook of advanced electronic and photonic materials and devices, in: H.S. Nalwa (Ed.), Ferroelectrics and Dielectrics, vol. 4, Academic, 2001.
[48] J. Luo, Z. Xie, J.W.Y. Lam, L. Cheng, H. Chen, C. Qui, H.S. Kwok, X. Zhan, Y. Liu, D. Zhu, B.Z. Tang, Chem. Commun. (2001) 1740.
[49] J. Chen, Z. Xie, J.W.Y. Lam, B.Z. Tang, Macromolecules 36 (2003) 1108.
[50] Y. Ren, J.W.Y. Lam, Y. Dong, B.Z. Tang, K.S. Wong, J. Phys. Chem. 109 (2005) 1135.
[51] J. Chen, B. Xu, Y. Cao, H.H.Y. Sung, I.D. Williams, B.Z. Tang, J. Phys. Chem. 109 (2005) 17086.
[52] S. Hai-Ching, F. Omrane, Y. Chih Jen, C. Ting-Yi, F. Claire, H. Muriel, W. Chung-Chih, R. Re'gis, J. Am. Chem. Soc. 128 (2006) 983.
[53] F. D'Amore, A. Zappettini, G. Facchini, S.M. Pietralunga, M. Martinelli, C. Dell'Erba, C. Cuniberti, D. Comoretto, G. Delle piane, Synth. Met. 127 (2002) 143.
[54] G.R. Meredith, Phys. Rev. B 15 (1981) 5522.